

CODA ATTENUATION FOR 4 TO 64 Hz IN THE CRUST
MEASURED AT ASHIO, JAPAN

Ioannis BASKOUTAS* and Haruo SATO**

* National Observatory of Athens, Seismological Inst.
118 10 Athens, Greece

** National Research Center for Disaster Prevention
Tennodai 3-1, Tsukuba, Ibaraki, Japan

ΠΕΡΙΛΗΨΗ

Υπολογίσθηκε η τιμή του Q_c^{-1} των ουρών των σεισμικών κυμάτων απ' τη χρονική εξασθένηση φιλτραρισμένων σειсмоγραμμάτων με βάση το μοντέλο απλής διασποράς.

Αναλύσαμε για το σκοπό αυτό σεισμικά δεδομένα απ' την περιοχή Ashio της επαρχίας Tochigi στην κεντρική Ιαπωνία, όπου η σεισμικότητα είναι υψηλή.

Οι τιμές του Q_c^{-1} σε μικρά χρονικά διαστήματα, περίπου 10 δευτερόλεπτα, μετά την ανάδυση των εγκαρσίων κύματων, που δίνουν την τιμή του Q_c^{-1} στον αβαθή φλοιό, βρέθηκαν να μικραίνουν σε σχέση με την συχνότητα από 2.5×10^{-2} στα 4Hz σε 6.0×10^{-4} στα 64Hz.

Οι τιμές του Q_c^{-1} στον αβαθή φλοιό και για συχνότητες κάτω από 24Hz είναι περίπου τρεις φορές μεγαλύτερες απ' ό,τι η τιμή που υπολογίστηκε για χρονικά διαστήματα μέχρι 100 δευτερόλεπτα και αντιστοιχεί στον φλοιό και ένα μέρος του πάνω μανδύα.

Γενικά η διαφορά των τιμών σε χαμηλές συχνότητες είναι μεγάλες αλλά υπάρχει τάση σύγκλισης στα 64Hz.

Η τιμή του εκθέτη n στη σχέση $Q_c^{-1} \approx f^n$ παίρνει την τιμή -0.98 για τους σεισμούς της ομάδας C και την τιμή -0.78 για τους σεισμούς της ομάδας D.

ABSTRACT

Coda attenuation Q_c^{-1} has been evaluated from the temporal decay of band-pass filtered seismograms based on the single scattering model. We analysed seismic data obtained at Ashio, Tochigi prefecture in central Japan, where seismic activity is very high in the crust. Q_c^{-1} evaluated from short lapse, time smaller than 10s, which sample the shallow crust, decreases in frequency from 2.5×10^{-2} at 4Hz to 6.0×10^{-4} at 64Hz. Q_c^{-1} of the shallow crust for frequencies smaller than 24Hz is about three times larger than Q_c^{-1} evaluated from coda of lapse time up to 100s, which corresponds to the crust and a portion of upper mantle. Difference is large in the low frequency, but both converge at 64Hz. The power of frequency is -0.98 and -0.78 for the shallow crust and the crust plus a portion of upper mantle, respectively.

INTRODUCTION

In high frequency seismology ($f > 1\text{Hz}$), the measurement of attenuation is difficult to accomplish mainly due to the sensitivity of seismic waves in this frequency band, to the earth structure (Chang and von Seggern 1980, Pulli, 1984). The statistical treatment of the heterogeneities of the earth medium may be the case to avoid the above difficulties.

Aki (1969) suggested that the coda waves are the result of backscattering from numerous randomly distributed heterogeneities in the crust and the upper mantle. Such heterogeneities can be considered as cracks, faults folds, density and velocity anomalies in the earth medium, ect.

Two extreme models have been proposed by Aki and Chouet (1975) to explain the characteristics of the coda waves. One is the single back scattering model, in which coda waves are considered as superposition of backscattered wavelets from discrete scatterers. This model assumes that scattering is a weak process. The second, the diffusion model, assumes that the seismic energy transfer as a diffusion (strong scattering) process. This model is based on the diffusion theory of Wesley (1965). Dainty and Toksoz (1981) have argued that diffusion model may be not appropriate for earthquakes, since the observed diffusion rise times are much shorter than that the theory predicts. Sato (1977) proposed the single isotropic scattering model for explaining the asymptotic behavior of coda waves at different stations. He considered coda waves only as scattered body waves and elastic energy is radiated spherically in the infinite elastic and isotropic medium.

In this study we applied the method of Sato (1977) to high quality data, obtained at Ashio station, to determine Q_c^{-1} in this region, especially in the shallow crust, and also in the crust plus a portion of the upper mantle. So far no precise measurement of Q_c^{-1} in the shallow crust has been succeeded, because it is necessary to install seismometers in the vicinity of the earthquake sources and also few observations have been reported for high frequency above 30Hz. Fortunately, in the Ashio region we succeeded to obtain such data. We believe that this analysis useful for understanding the physical difference between the shallow crust and a deeper region.

METHOD

On the base of the single isotropic model, Sato (1977) derived the coda energy density at frequency f as follows:

$$E_s(r, f, t) = [N_0(f) W_0(f) / (4\pi r^2)] K(\alpha) \exp(-Q_c^{-1} 2\pi f t) \quad (1)$$

where r is the hypocentral distance and t is the lapse time measured from origin time; $\alpha = t/t_e$ where t_e the S -wave travel time; N_0 is the effective scattering coefficient; W_0 is the total S -wave energy spherically radiated from the source. It means that coda wave consist of scattered waves from

ellipsoid shells. The function $K(\alpha)$ is given by

$$K(\alpha) = (1/\alpha) \ln[(\alpha+1)/(\alpha-1)] \quad (2)$$

which asymptotically behaves (Sato 1977) as

$$K(\alpha) \approx 2(t_e/t)^2 \quad \text{for } t \gg t_e \quad (3)$$

From (1) and (3) we get

$$E_s(r, f, t) \exp(-Q_c^{-1} 2\pi f t) / t^2 \quad (4)$$

Relation (4) corresponds to Aki and Chouet's (1975) single back scattering model.

Energy density of coda waves is proportional to the root mean square coda amplitude $A(r, f, t)$ of the band pass filtered seismogram at a center frequency f and therefore from (4) we get

$$A(r, f, t) \exp(-Q_c^{-1} \pi f t) / t \quad (5)$$

Taking the logarithm of (5)

$$\log(A t) = C(f) - Q_c^{-1}(f) (\pi f \log e) t \quad (6)$$

Applying this relation to the observed data, we directly evaluate the linear gradient of $\log(A t)$ against lapse time, which is equal to $Q_c^{-1} \pi f \log e$.

DATA AND ANALYSIS

Ashio station (36.63 °N, 139.46 °E, altitude 755m) is located on the Western border of Tochigi prefecture, central, Japan, as shown by a solid triangle in Fig. 1. The Ashio region is known by its high seismicity in the crust and is located on the volcanic front.

Most of the seismic events we analysed belong to the shallow seismicity (group C in fig. 1), and other several events (group D) belong to the subducting Pacific plate, which were analysed for the comparison with Aki (1980)'s results. Location and parameters of the events used in this study are reported by the NRCDP bulletin and are listed in Table I. For an event which has no parameters, the origin time is calculated using the S-P time difference. The local magnitude of the earthquakes range between 1.0 to 3.2. Earthquakes occurring near Ashio station mostly have a magnitude less than 3.0, and no earthquake with magnitude larger than 5.0 occurred in the area for decades (Sekiya, 1973). The horizontal and vertical (E-W) distribution of hypocenters of the earthquakes used in this analysis are shown in Fig. 1(a), (b), respectively.

The horizontal (N-S) component seismograph the recordings of which we used in the present study used is a moving coil type of natural frequency 1Hz. The frequency response is flat in velocity up to 300Hz. The recordings were band-pass filtered with an electric circuit serially

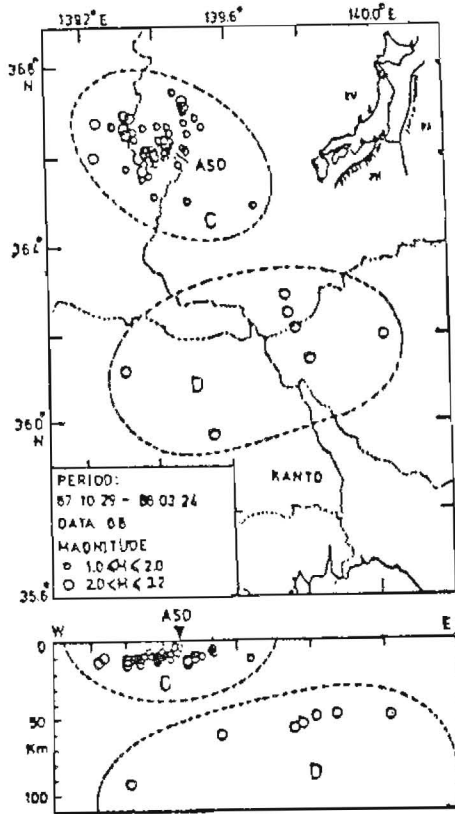


Fig. 1. Epicenter distribution of earthquakes used in this analysis, (b) vertical (E-W) cross section of hypocenters. Solid triangle shows the location of Ashio station (ASO). A solid box in the upper right figure shows Ashio area.

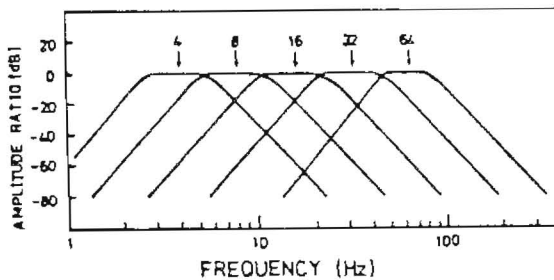


Fig. 2. Frequency response of band-pass filters used in the analysis.

Table I

Events recorded at Ashio station and their parameters routinely determined by the NRCDP network.

No.	Date	Origin Time	Lat. (°N)	Long. (°E)	Depth Km	Magn.
1	87 1029	13:24:35.4	36.67	139.47	7.0	1.9
2	87 1030	07:33:38.6	36.63	139.54	9.9	1.9
3	87 1112	07:26:29.1	36.63	139.46	8.5	1.5
4*	87 1115	16:38:30.6	36.21	139.79	54.1	2.8
5*	87 1121	02:46:17.4	36.13	139.32	93.6	3.2
6*	87 1125	21:21:16.5	35.97	139.56	60.9	2.8
7	87 1127	00:37:06.2	36.66	139.33	10.3	1.9
8	87 1129	20:19:00.9	36.49	139.64	10.9	1.8
9*	87 1129	23:11:36.6	36.16	139.85	47.8	2.7
10	87 1202	22:15:22.6	36.62	139.49	9.9	1.9
11	87 1203	10:17:32.7	36.62	139.49	10.8	2.2
12	87 1206	05:01:27.1				
13	87 1210	07:11:38.0	36.63	139.47	7.3	1.6
14*	87 1210	07:51:33.8	36.20	140.02	49.0	2.6
15	87 1212	01:37:17.6	36.58	139.37	9.5	2.2
16	87 1214	19:28:15.8	36.62	139.44	6.7	1.7
17	87 1216	06:15:34.4	36.56	139.37	8.9	2.2
18	87 1231	12:15:51.8	36.62	139.45	7.6	1.6
19	88 0101	19:14:10.2	36.62	139.37	5.3	1.0
20	88 0106	14:37:32.2				
21	88 0107	04:39:16.0	36.59	139.34	7.9	1.8
22	88 0109	08:45:53.1	36.62	139.50	11.7	2.7
23	88 0110	23:32:00.0	36.58	139.40	7.9	1.7
24	88 0114	09:39:23.4	36.60	139.40	10.1	2.2
25	88 0114	11:34:44.6	36.60	139.40	7.0	2.2
26	88 0114	11:36:15.3	36.60	139.38	10.6	2.8
27	88 0114	11:37:52.3	36.60	139.40	6.7	2.3
28	88 0114	11:42:32.1	36.61	139.40	9.3	1.9
29	88 0114	11:54:12.0	36.50	139.53	5.0	1.7
30	88 0114	13:24:08.2	36.59	139.40	5.7	1.3
31	88 0115	18:29:06.6	36.61	139.38	10.8	2.4
32	88 0115	18:52:45.9	36.61	139.38	10.2	1.9
33	88 0115	20:38:27.3	36.60	139.40	10.3	2.1
34	88 0115	23:37:22.5	36.60	139.38	10.0	1.8
35	88 0116	01:35:16.9	36.59	139.48	10.1	1.8
36	88 0112	00:16:06.3	36.67	139.49	8.5	1.7
37	88 0123	02:30:06.8	36.61	139.43	7.4	2.0
38	88 0124	03:25:41.0	36.61	139.44	5.6	1.6
39	88 0126	01:01:08.3	36.62	139.44	6.8	1.8
40	88 0126	02:39:19.5	36.62	139.43	10.1	2.0
41	88 0126	14:34:35.5	36.60	139.44	3.2	1.8
42	88 0127	15:53:03.4	36.66	139.49	3.9	2.1
43	88 0128	04:11:50.6	36.60	139.39	9.4	2.2
44	88 0131	16:26:11.5	36.57	139.38	6.2	2.0
45	88 0131	19:39:57.7	36.71	139.42	8.9	2.1
46	88 0201	15:52:22.1	36.61	139.44	22.1	1.6
47	88 0201	21:59:55.8	36.63	139.45	6.1	1.6
48	88 0219	03:48:07.4	36.57	139.34	8.7	2.0
49	88 0221	22:26:08.2	36.55	139.37	7.5	1.8
50	88 0223	04:46:19.0	36.68	139.35	9.1	2.1
51	88 0223	06:05:38.1	36.68	139.34	10.1	2.1
52	88 0227	19:06:07.3				
53	88 0228	00:34:00.3	36.68	139.60	15.0	1.9
54	88 0228	23:36:11.1				
55	88 0303	22:04:01.1				
56	88 0306	13:47:33.2				
57	88 0312	01:31:11.9	36.63	139.51	8.7	1.9
58	88 0312	16:13:13.3	36.58	139.22	11.1	2.6
59	88 0313	08:00:45.8	36.63	139.30	10.9	2.1
60	88 0314	17:21:12.7	36.62	139.46	9.1	1.8
61	88 0315	04:08:55.5	36.74	139.48	7.7	1.8
62	88 0315	06:39:15.5	36.74	139.49	7.6	2.2
63	88 0316	04:23:11.5	36.63	139.30	12.5	2.6
64*	88 0317	18:59:14.6	36.25	139.77	56.4	2.6
65	88 0319	16:18:36.7	36.65	139.34	10.0	2.1
66	88 0320	16:47:23.8				
67	88 0321	16:13:22.0				
68*	88 0324	10:33:08.9	36.14	139.82	48.3	2.8

Events with asterisk belong to group D.

composed of an octave-width band-pass filter (BPF), root mean square (RMS) amplifier and a logarithmic amplifier (LOG). The electric circuit was designed for the coda decay analysis by Sato (1986). The BPF-RMS-LOG output was recorded on paper with chart speed of 10mm/s. Fig. (2) shows overall frequency response of the BPF-RMS-LOG circuit.

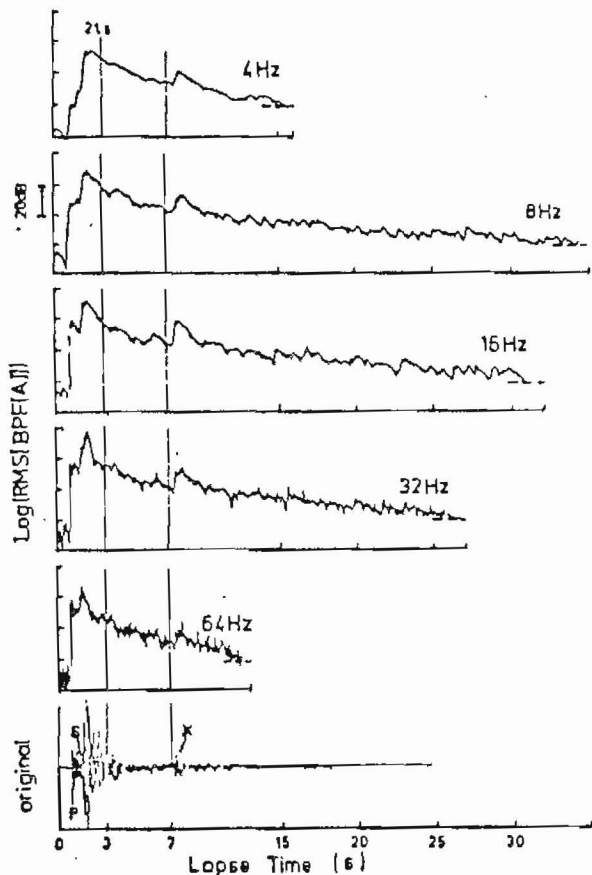


Fig. 3. Example of band-pass filtered RMS amplitude versus lapse time at each frequency band.

Fig. (3) shows an example of the BPF-RMS-LOG output versus lapse time, t , in sec. The starting point for the analysis was chosen after $2t_s$, as the model restricts us for the generation of coda waves. The end point is visually chosen before the amplitude of the signal becomes equal to the noise level. RMS amplitudes for in each band are measured across the time series every 0.5 or 1.0s, in order to smooth out irregularities in amplitude. Measurements of coda decay amplitude before a sharp reflection phase following direct S-waves around up to 10s allowed us to

obtain the Q_c^{-1} at very shallow part of the crust. This reflection phase (referred as X in fig 3.) was studied by Mizue et al., (1982). For lapse time up to 100s we were able to measure Q_c^{-1} for a larger and deeper zone. The lapse time is related to the sampled region responsible for the generation of coda waves. Scatterers are considered to be distributed on the surface of an ellipsoid. According to our model, coda waves at lapse time up to 10s sample a sphere of radius of about 18km, assuming an S-wave velocity of 3.5km/s. The greater epicentral distance and lapse time, the larger the corresponding sampled region. We applied relation (6) to the data and obtained the Q_c^{-1} values by the least square method.

RESULTS AND DISCUSSION

Coda Q_c^{-1} values for the shallow crust beneath the Ashio station were determined at five frequency bands for group C. From very short lapse time up to around 10s, Q_c^{-1} has been found to decrease almost monotonically from $2.5 \times 10^{-2} \pm 3.6 \times 10^{-3}$ at 4Hz to $6.0 \times 10^{-4} \pm 2.0 \times 10^{-4}$ at 64Hz (left column of Table II).

Table II - Values of Q_c^{-1}

Freq.	Shallow Crust ($2t_s - t - 10a$)		Crust plus Upper Mantle ($2t_s - t - 100a$)		Deep events Group D
	Group C		Group C		
4Hz	$2.5 \times 10^{-2} \pm 3.6 \times 10^{-3}$	(11)	$8.4 \times 10^{-3} \pm 3.9 \times 10^{-3}$	(53)	$3.6 \times 10^{-3} \pm 5.1 \times 10^{-4}$ (7)
8Hz	$1.1 \times 10^{-2} \pm 3.6 \times 10^{-3}$	(13)	$3.1 \times 10^{-3} \pm 1.5 \times 10^{-3}$	(61)	$2.1 \times 10^{-3} \pm 1.4 \times 10^{-4}$ (7)
16Hz	$4.4 \times 10^{-3} \pm 1.8 \times 10^{-3}$	(12)	$1.5 \times 10^{-3} \pm 6.0 \times 10^{-4}$	(62)	$1.1 \times 10^{-3} \pm 1.8 \times 10^{-4}$ (7)
32Hz	$2.1 \times 10^{-3} \pm 7.0 \times 10^{-4}$	(61)	$9.0 \times 10^{-4} \pm 2.0 \times 10^{-4}$	(61)	$7.5 \times 10^{-4} \pm 1.2 \times 10^{-4}$ (7)
64Hz	$6.0 \times 10^{-4} \pm 2.0 \times 10^{-4}$	(10)	$6.0 \times 10^{-4} \pm 2.0 \times 10^{-4}$	(53)	$3.2 \times 10^{-4} \pm 3.3 \times 10^{-4}$ (7)

Number in each parenthesis means the number of events.

Because of the restriction of the models for the generation of coda waves and because of the presence of the reflection phase, it means from lapse time $2t_s$ and before the reflection phase, the number of the examined events were reduced to 10-13. Kosuge (personal communication, 1988) also obtained such a high value of Q_c^{-1} for events with very short epicentral distance i.e. 1.3km, in western Nagano area, Japan. Taking into account all the coda duration, the sampled area becomes larger and deeper. Thus we were able to obtain Q_c^{-1} for the crust plus a portion of the upper mantle from group C. In this case the mean values of Q_c^{-1} have been found lower and decreasing from $8.4 \times 10^{-3} \pm 3.9 \times 10^{-3}$ at 4Hz to $6.0 \times 10^{-4} \pm 2.0 \times 10^{-4}$ at 64Hz (middle column of Table II). Finally a group of more distant and deeper events were analysed separately. Those events are shown in Fig. (1) as group D. In this case Q_c^{-1} values agree well with the

values obtained by Aki(1980) for the Kanto area in the lithosphere. Unfortunately we can not compare our results at the high frequency band of 64Hz, since there are not analysed data at this high frequency band. In Table II the mean values and standard deviation of Q_c^{-1} are shown for each frequency band. The results from all the three groups are shown in Fig. (4) on Aki's conjecture diagram (Aki, 1980) in order to compare them with Q^{-1} of S and coda waves in the lithosphere at several different regions in the world.

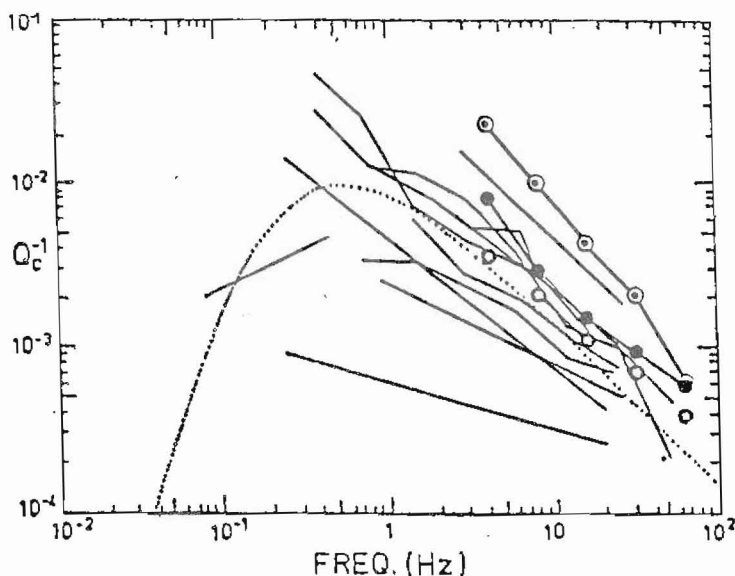


Fig. 4. Observed relation of Q_c^{-1} of S and coda waves frequency obtained at several parts of the world (added to Figure 12 of Sato 1984). Open circles correspond to Q_c^{-1} in the shallow crust, solid one correspond to Q_c^{-1} in the crust plus a portion of upper mantle (both belong to group C). Circles with asterisk correspond to Q_c^{-1} of group D. The dotted line was predicted theoretically predicted by Sato (1984).

The upper open circles correspond to the Q_c^{-1} in the shallow crust, lower solid circles correspond to the deeper zone for earthquakes of group C. Circled asterisks correspond to the Q_c^{-1} obtained from the set of the deeper and more distant events (group D) which are located beneath the Kanto plain area. The dotted line represents the theoretical curve predicted by Sato (1984).

Looking at Fig. (4) we can see that Q_c^{-1} values tend to converge at high frequencies (64Hz) and diverge at low frequencies. This convergence was reported first by Aki (1980) after reviewing results from Japan, California, Hawaii, Central and Eastern US and Kamchatka. Several

researchers suggest that if the weak scattering holds then Q_c^{-1} at shallow depths could be the average Q_m^{-1} at the same depth (Aki, 1980, Roecker, et al., 1982).

The clear frequency-dependent behavior of Q_c^{-1} has been found here, as several researchers have reported (Aki and Chouet, 1975, Rautian and Khalturin, 1978, Rovelli, 1981, Del Pezzo et al., 1983, Van Eck, 1988). The data fit to a power law of the form $Q_c^{-1} \approx f^n$. In our case $n = -0.78$ for the crust plus the portion of the upper mantle and $n = -0.98$ (4-32Hz) or $n = -1.3$ (4-64Hz) for the shallow crust.

We may think several reasons for higher Q_c^{-1} in the shallow crust. High seismicity in the area means a large amount of cracks in the shallow crust, which may increase the absorption. The second, scattering is much stronger in the shallow crust than those in the deeper portion. It makes bigger amplitude in early coda than the latter part of coda. This is higher Q_c^{-1} in the shallow crust. The third possibility is that if we consider a clustering of cracks, then the fractal dimension becomes smaller and therefore the multiple scattering effects are predominant in the early coda (Sato, 1988). This will make coda decay more steeper, that is higher Q_c^{-1} , where Q_c^{-1} is an indicator of anomaly in steepness of coda decay.

To understand what exact what does Q_c^{-1} mean and how to separate from intrinsic attenuation is a task to be investigated more in the future, as other problems related to the study of such promising subject, like coda wave attenuation are.

ACKNOWLEDGEMENTS

One of the authors (I.B.) visit to BRI and NRCDP in Tsukuba, Japan, was supported by Japan International Cooperation Agency. He is grateful to Prof. J. Drakopoulos for giving him the opportunity to visit Japan. This work was partially supported by the project of Science and Technology Agency entitled "Study of earthquakes, fractures and wave propagation in inhomogeneous structure of the earth medium." We much appreciate Prof. N. N. Andrassy's suggestions and careful reading of the manuscript.

REFERENCES

- Aki, K., 1969. Analysis of the seismic coda of local earthquakes as scattered waves. *J. Geoph. Res.*, 74, 615-631.
- Aki, K., 1980. Scattering and attenuation of shear waves in the lithosphere. *J. Geoph. Res.*, 85, 6496-6504.
- Aki, K., and Chouet, B., 1975. Origin of coda waves: source, attenuation and scattering effects. *Geoph. Res.*, 80, 3322-3342.
- Chang, A., and D. H. von Seggern, 1980. A study of amplitude anomaly and m bias at LASA subarrays. *J. Geoph. Res.*, 85, 4811-4828.
- Dainty, A., and M. N. Toksoz, 1981. Seismic codas on the

- earth and the Moon: a comparison. *Phys. Earth Planet. Interiors.*, 26, 250-260.
- Del Pezzo, E., F., and M., Martini, 1983. Attenuation of short period seismic coda waves in the Aolian islands-Southern Italy. *Boll. Geof. Teor. Appl.*, XXV, 97, 45-51.
- Mizoue, M., Nakamura, I., and T., Yokta, 1982. Mapping of an unusual crustal discontinuity by microearthquakes reflection in the earthquake swarms area near Ashio, northern part of Tochigi prefecture, Central Japan. *Bull. Earth. Inst. Tokyo Uni.*, 57, 653-686.
- Pullii, J. J., 1984. Attenuation of coda waves in New England. *Bull. Seism. Soc. Am.*, 74, 1149-1166.
- Rautian, T. G., V. I. Khalturin, 1978. The use of the coda for determination of the earthquake source spectrum. *Bull. Seism. Soc. Am.*, 68, 923-948.
- Roecker, S. W., B. E. Turker, J. L. King, and D. Hatzfeld, 1982. Estimates of Q in central Asia as a function of frequency and depth using the coda of locally recorded earthquakes. *Bull. Seism. Soc. Am.*, 72, 129-149.
- Rovelli, A., 1982. On the frequency dependence of Q in Friuli from short-period digital records. *Bull. Seism. Soc. Am.*, 72, 2369-2372.
- Sato, H., 1977. Energy propagation including scattering effects, single isotropic scattering approximation. *J. Phys. Earth*, 25, 27-41.
- Sato, H., 1984. Attenuation and envelope formation of three component seismograms of small local earthquakes in randomly inhomogeneous lithosphere. *J. Geoph. Res.*, 91, 2049-2061.
- Sato, H., 1986. Regional study of Q_c^{-1} in Kanto district, Japan. (In Japanese). *Zisin*, 39, 241-249.
- Sato, H., 1988. Is the single scattering model invalid for the coda excitation at long lapse time? *Pageoph.* (in press).
- Sekiya, H., 1973. On the seismic activity in the southern part of Kanto (Relation between the earthquake swarms and other large earthquakes), (in Japanese). *Rep. Coord. Commit. Earthq. pred.*, 10, 36-39.
- Van Eck, T., 1988. Attenuation of coda waves in the Dead Sea region. *Bull. Seism. Soc. Am.*, 78, 770-779.
- Wesley, J. P., 1965. Diffusion of seismic energy in the near range. *J. Geophys. Res.*, 70, 5099-5106.